International Journal of Engineering and Geosciences
https://dergipark.org.tr/en/pub/ijeg
e-ISSN 2548-0960

Design of ultra-wide band dual-polarized quad ridged horn antenna for obstacle penetrating radar imaging applications

Betül Yılmaz[*1]

[1]*Mersin University, Department of Electrical-Electronics Engineering, Türkiye*

Keywords
Antenna Design
Horn Antenna
CAD
Radar Imaging
Quad ridged Horn Antenna

Research Article
DOI: 10.26833/ijeg.1053213

Received: 04.01.2022
Accepted: 04.02.2022
Published: 13.04.2022

Abstract

In this study, a high-gain and dual-polarized Quad Ridged Horn Antenna (QRHA) is proposed and designed to be used in Obstacle Penetrating Imaging Radar (OPIR) applications. The quad ridged design is developed and then optimized by using the antenna design simulator software; CST Microwave Studio. The antenna parameters including the center frequency, frequency bandwidth and the antenna radiation pattern beam width are considered based on the requirements of OPIR applications. The final design is obtained for the center frequency of 2.785 GHz with a -10 dB bandwidth of at least 2.5 GHz. The final designed QRHA is able to provide a gain of 12.4 dB with a beam width of 36° at the center frequency of 2.785 GHz.

1. Introduction

As the new antenna applications are emerging thanks to improvements in signal processing algorithms [1] and developments on near field antenna application such as indoor radar imaging and car-to-car communication, the need for ultra-wideband (UWB) antenna technologies are increasing vastly. Among these applications, near-field radar imaging technologies [2] have also gaining much attention thanks to developments in microwave electronic circuitries [3-5]. For such applications including thru-wall imaging radar (TWIR) [6-8] and ground-penetrating radar (GPR) [9-11] or more generally obstacle penetrating imaging radar (OPIR), the scene is at the near-field of the radar antenna. Therefore, this necessitates the resolution of the image to be on the order of a few centimeters or less. This requirement; of course, forces the bandwidth of the radar antenna to be as large as possible [12] and preferably have UWB feature.

Some candidate UWB antennas including biconical antenna [13], helical antenna [14], log-periodical antenna [15-16], Vivaldi antenna [17] and ridge-horn antenna [18], have been well studied by many researchers. Among them, Vivaldi Antenna, Antipodal Vivaldi microstrip patch antenna, and double ridged horn antenna are widely considered due to suitable for OPIR applications since they have the attractive features such as high gain, relatively narrow beam width, directional antenna pattern and UWB operation. While patch antennas have the advantage of being compact, light and small [19-21]; their frequency bandwidth features are not that good when compared to horn antennas.

We have previously presented an optimized design of double ridged horn antenna (DRHA) that can be practically used for OPIR applications [22]. This antenna had the ability to offer UWB usage with a directional pattern that was specifically designed and produced for TWIR practices. For the recent couple of years, researchers have shown that the use of multiple polarization could increase the probability of detection and also facilitate the classification of the targets [23-24].

In this paper, a novel dual-polarized Quad Ridged Horn Antenna (QRHA) is designed for the OPIR applications such as GPR and TWIR. In the next section, the basic design steps are shared for the dual-polarized QRHA. The full EM simulation of the antenna is performed by the commercially available CST® Microwave Studio [25]. The optimization parameters and also the optimized design of the targeted antenna are

* **Corresponding Author**
*(betuly@mersin.edu.tr) ORCID ID 0000-0001-7404-8312

Cite this article
Yılmaz, B. (2023). Design of ultra-wide band dual-polarized quad ridged horn antenna for obstacle penetrating radar imaging applications. International Journal of Engineering and Geosciences, 8(1), 76-82

given in this section as well. In the third section, the antenna parameter fulfillments are presented to reflect the successfulness of the designed antenna. The final section is dedicated to the conclusion of the work and the possible usage of the designed antenna.

2. Design and the CST Simulation of Dual-Polarized Qrha

The proposed the dual-polarized QRHA is designed and simulated with commercially available full-wave electromagnetic (EM) simulator tool of CST Microwave Studio [25]. The required characteristics of the designed antenna are listed below:

i. An operational bandwidth was aimed to be at least 2.5 GHz around center frequency of 2.75 GHz.
ii. Beam-width of the main lobe was objected to be approximately 30° to 40° at the center frequency of the bandwidth.
iii. The size of the complete antenna is to be compact. Our goal was to have a design to be shorter than 35 cm.

First, a preliminary design based on the double ridged horn antenna theory Yılmaz and Özdemir [22] is applied to be able to attain a starting point before optimization. During the optimization, the Trust Region Framework algorithm is utilized inside CST such that finite difference accuracy value of 0.01 had been targeted. Then, the QRHA is optimized based on the antenna parameter constraints that are listed above using the optimization tool of CST Microwave Studio. As a result, the final design for the QRHA is obtained as shown in Fig. 1. The perspective, side, front, inner and, back views of the final QRHA is given in Fig. 1 (a), (b), (c), (d), and (e), respectively.

The critical dimensions of the final, designed QRHA are listed in Table 1.

Table 1. Dimension parameters of QRHA

Parameter	Description	Value (mm)
W_L	Wave-guide length	161.61
H_L	QRHA total length	319.55
A_w	Aperture width	227.36
A_h	Aperture height	224.00
R_w	Ridge width	10.68
L_d	Ridge separation	11.65
W_w	Wave-guide width	67.96
W_h	Wave-guide height	67.96

3. Simulation results

Based on the final optimized design parameters that are listed in Table 1, the QRHA is taken into simulation using CST. All of the critical antenna parameters are obtained and shared below:

The return loss performance of the QRHA is given for both co-polarization and cross polarization cases in Fig. 2 that also indicate the practical operational band width of the antenna.

In Fig. 2(a), co-polarization returns loss parameters of S_{11}, and S_{22} are given between 1 to 6 GHz. It can be easily noted from the figure that the -10 dB frequency bandwidth of the designed QRHA is from 1.47 GHz to 4.1 GHz that gives us a bandwidth of approximately 2.63 GHz at the center frequency of 2.785 GHz. Therefore, the fractional bandwidth is approximately equal to

$$B_{fr} = \frac{B}{f_c} = \frac{2.63\ \text{GHz}}{2.785\ \text{GHz}} = 94.43\% \qquad (1)$$

Above results obviously show that the designed QRHA yields an attractive UWB feature. In Fig. 2(b), the cross-polarization isolation plots; that is S_{21}, S_{12} of the designed antenna. From the figure, one can easily notice that the isolation between the dual-polarization ports of QRHA is successfully low; providing isolation power levels always less than -28.8 dB for all the frequencies within the bandwidth. On average, isolation power is around -34.8 dB inside the operational bandwidth.

In Fig. 3, the Voltage Standing Wave Ratio (VSWR) performance of the designed QRHA is given. In Fig. 3(a), VSWR of port 1 is plotted; where as in Fig. 3(b), that of port 2 is drawn. Both graphs show that VSWR is always less than 2 for the defined frequency bandwidth from 1.47 GHz to 4.1 GHz as expected.

In Fig. 4, far-field gain patterns at the center frequency of 2.785 GHz are given. When each port is used as stand-alone which means that the other port is not activated, the far field gain pattern of port #1 and port #2 are plotted in Fig. 4(a), and (b), respectively. It can be seen that the gains at the center frequency of operation is around 12.4 dBi for both ports when they are used in linear polarization mode of either Vertical (V) or Horizontal (H). When the designed QRHA is used in the circular polarization (CP), corresponding far-field gain patterns are given in Fig. 4(c) and (d), for the right-hand circular polarization (RHCP) and the left-hand circular polarization (LHCP), respectively. It can also be seen from the figure that the gains for both RHCP and LHCP are about the same performance of 12.4 dBi.

To evaluate the beam widths of the main beam of the designed QRHA, -3dB beam width analysis along the both E-plane and H-plane directions was performed thru the 2D far-field gain patterns at the center frequency of 2.785 GHz as depicted in Fig. 5. In Fig. 5(a) and (b), -3dB beam widths for linear polarization cases of H-plane and E-plane patterns of port #1 is plotted for the maximum radiation angle cut-direction, respectively. It can be easily read from the figures that half power beam width (HPBW) performances are resulted to be 41.1°, and 31.3° for port #1's H-plane and E-plane patterns, respectively. Similar analysis was also done for port #2 as well. In Fig. 5(c) and (d), -3dB beam widths for H-plane and E-plane patterns of port #2 is depicted for the maximum radiation angle cut-direction, respectively. It can also be referred from the figures that HPBW performances are measured to be 41.1°, and 31.2° for port #2's H-plane and E-plane patterns, respectively that are very similar to the ones for the port #1. All of these 2D far-field radiation patterns in Fig. 5 clearly demonstrate that this antenna can be practically used in OPIR applications since it can produce the desired HPBW performances of around 30° to 40°.

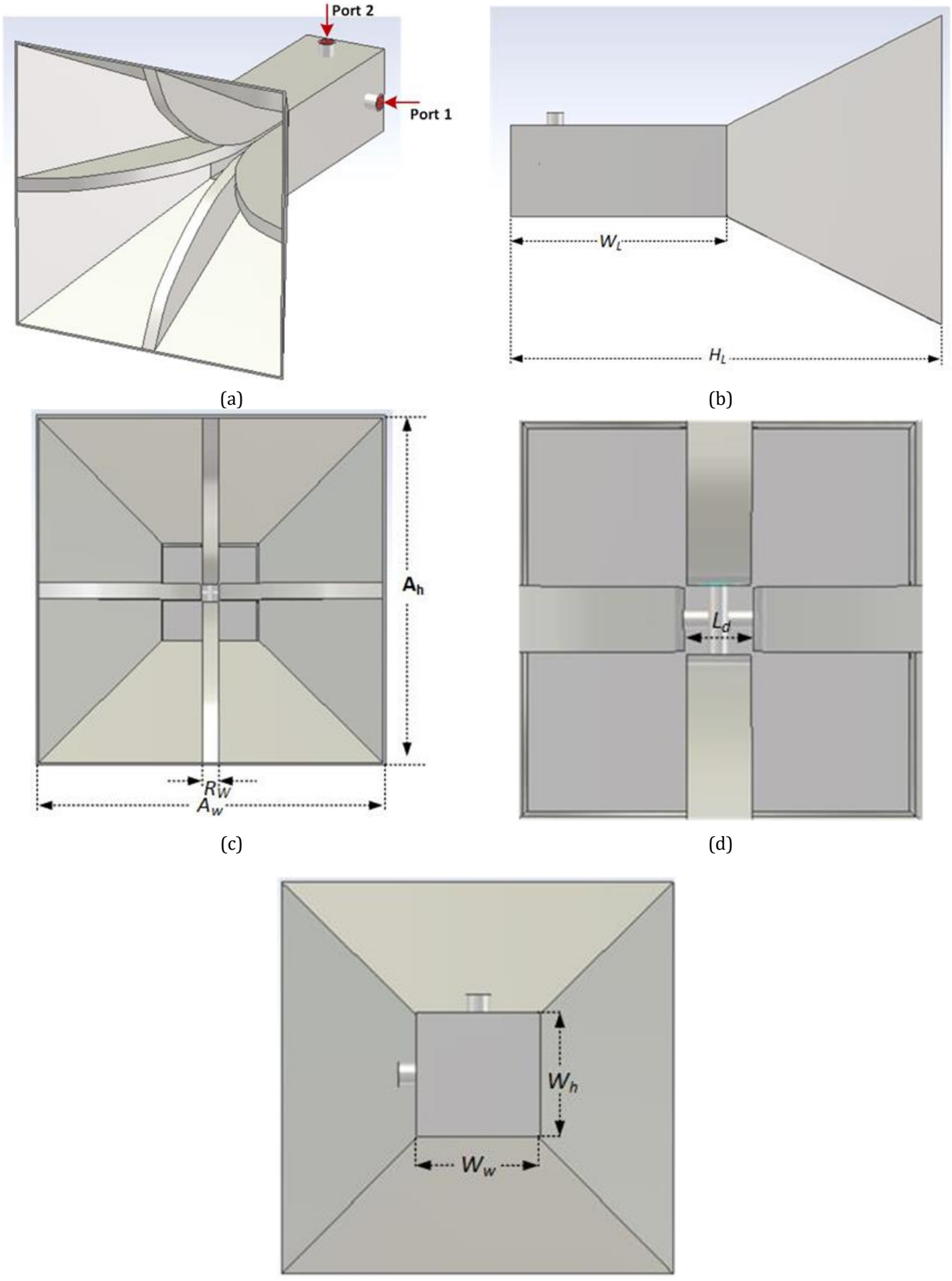

Figure 1. Designed QRHA with dimensions (a) perspective view, (b) side view, (c) front view, (d) a detailed view of the parameter for the width of the ridgeds, (e) back side

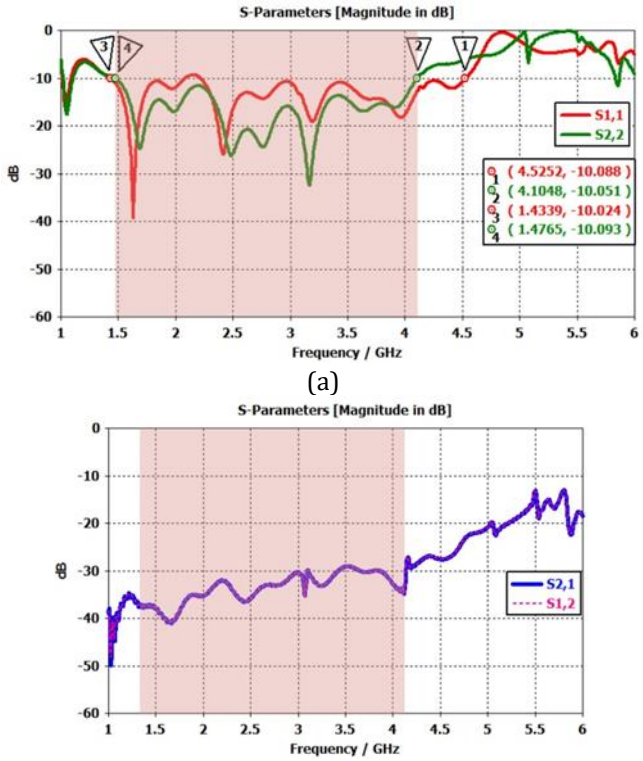

Figure 2. S-Parameters plots of the designed QRHA: (a) S_{11}, and S_{22} and (b) S_{21}, and S_{12}

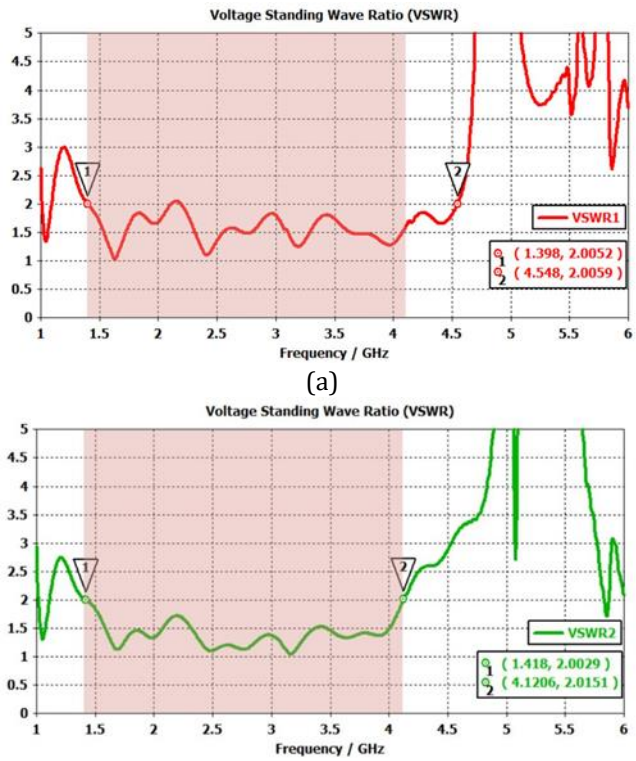

Figure 3. Voltage Standing Wave Ratio (VSWR) Results of the QRHA (a) for port 1, (b) for port 2

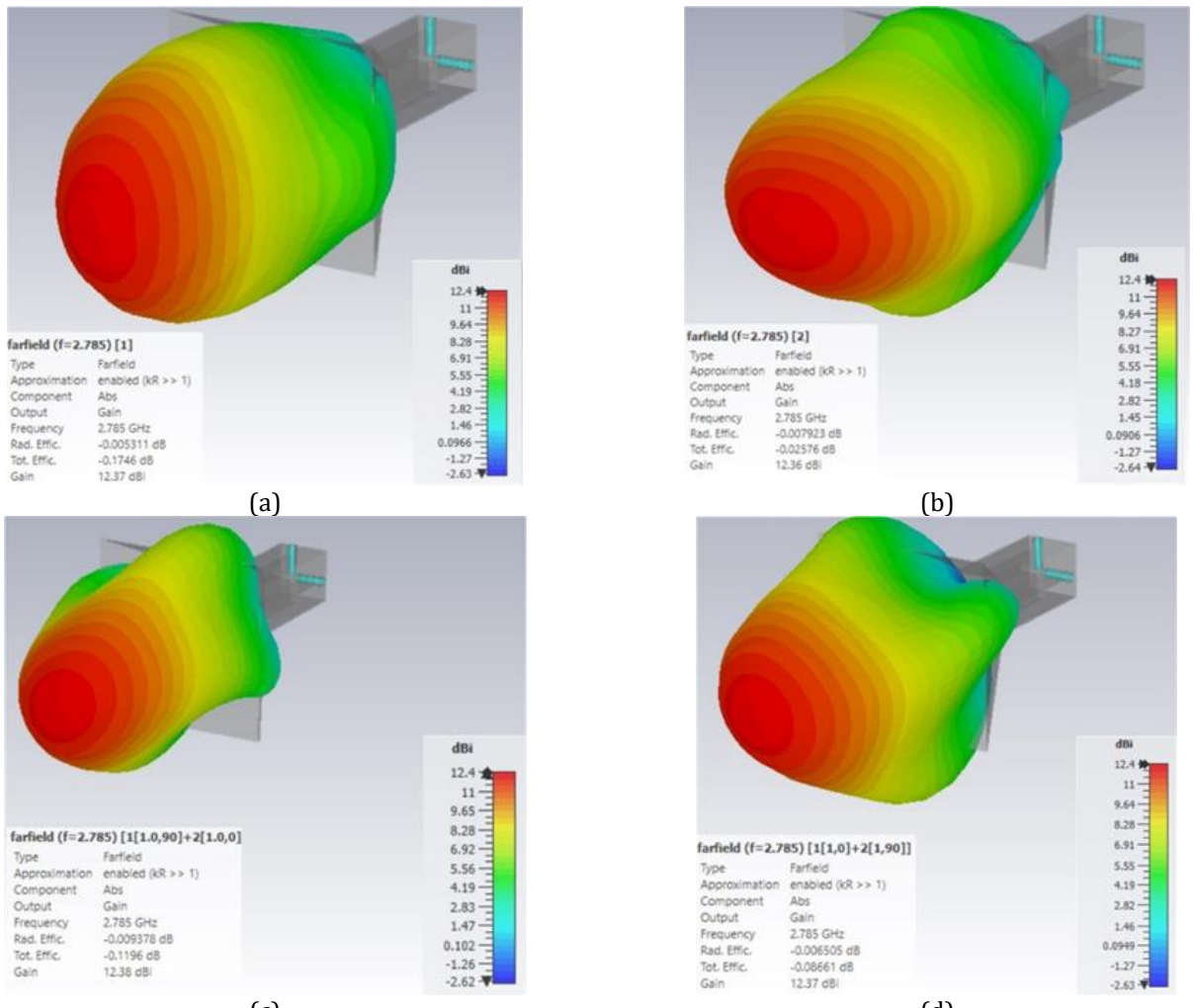

Figure 4. Far-field gain patterns at the center frequency of 2.785 GHz for (a) port #1, (b) port #2, (c) RHCP, and (d) LHCP

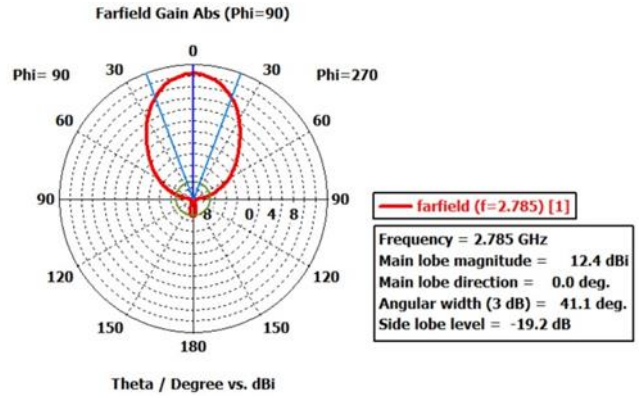

(a)

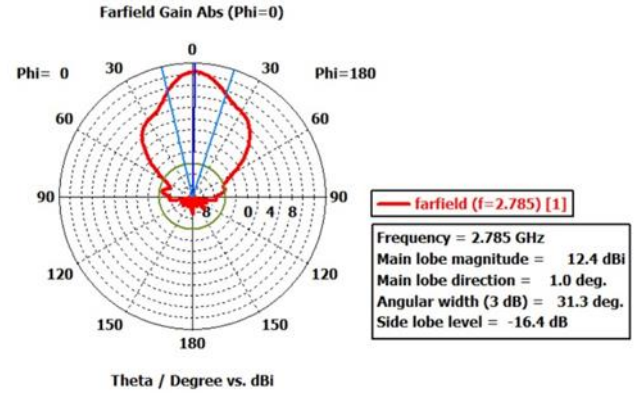

(b)

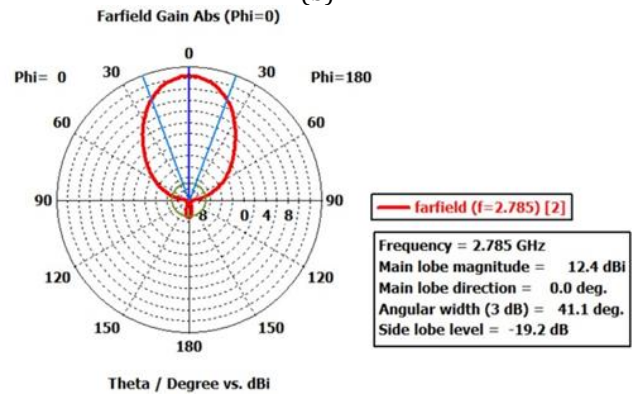

(c)

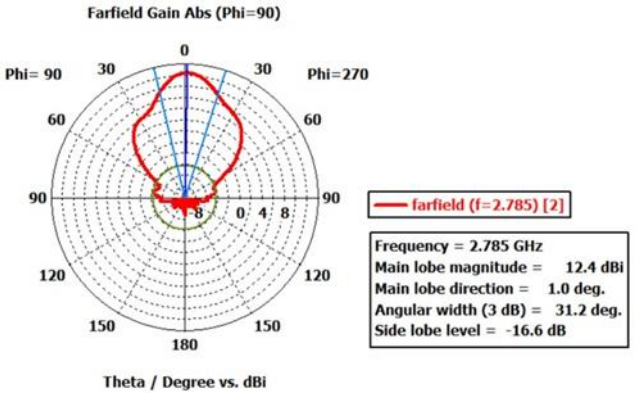

(d)

Figure 5. 2D Far-field radiation pattern cuts at 2.785 GHz in polar representation: (a) port #1 H-plane pattern, (b) port #1 E-plane pattern, (c) port #2 H-plane pattern, and (d) port #2 E-plane pattern

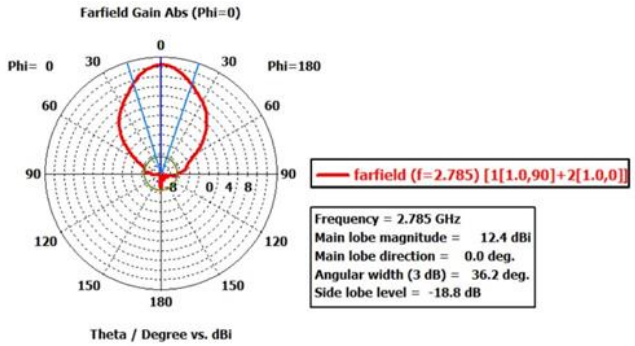

(a)

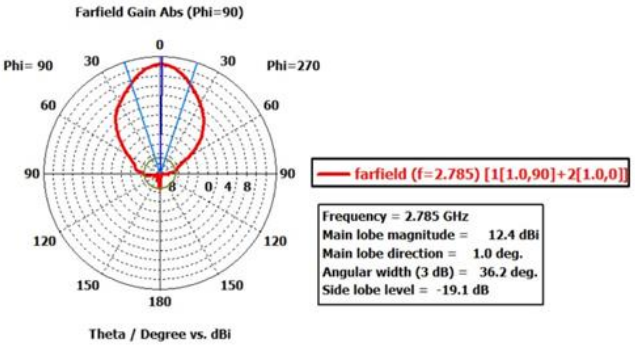

(b)

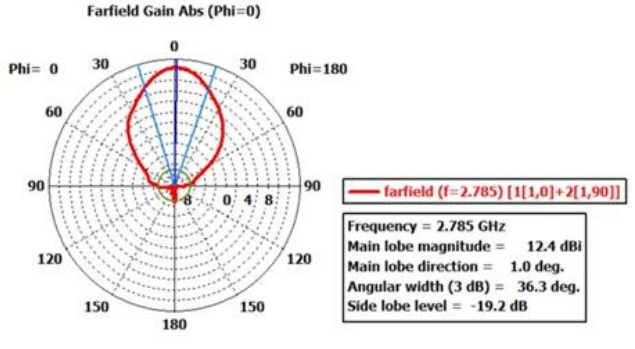

(c)

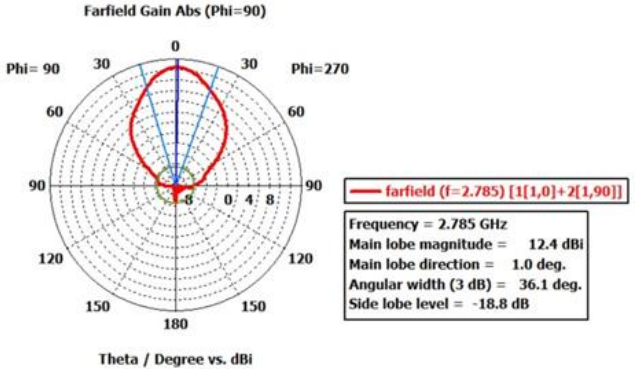

(d)

Figure 6. 2D Far-field radiation pattern cuts at 2.785 GHz in polar representation: (a) LHCP in x-z plane, (b) LHCP in y-z plane, (c) RHCP in x-z plane, (d) RHCP in y-z plane

In a further study, HPBW analysis was also performed for the CP usage of the designed QRHA. To achieve this, both ports are simultaneously activated while one of the ports is 90° in advance with respect to other port to yield LHCP or RHCP operation of the designed QRHA.

First, 2D far-field radiation pattern cuts of LHCP case at the center frequency of 2.785 GHz is considered thru Figs. 6(a) and 6(b). Fig. 6(a) represents the 2D far-field RHCP radiation pattern cut at $y = 0$ plane yielding a HPBW of 36.2° while, Fig. 6(b) stands for the same LHCP radiation pattern cut; but this time at $x = 0$ plane providing a HPBW of 36.2°. In Fig. 6(c) represents the 2D far-field RHCP radiation pattern cut at $y = 0$ plane with a HPBW performance of 36.3°. Whereas, Fig. 6(c) yields a HPBW of 36.1° for the same RHCP radiation pattern cut; but this time at $x = 0$ plane. Again, CP operation of the designed QRHA can provide directional usage of the antenna around 36° that is almost the mid-way of the design parameter.

4. Conclusion

In this study, a high-gain and dual-polarized horn antenna has been designed and optimized and to be practically used in OPIR applications. The final, optimized QRHA can be preferred for such practices thanks to its attractive antenna parameters that are validated by CST simulations. First of all, the final QRHA can provide a frequency band width of 2.63 GHz around the center frequency of 2.785 GHz providing an UWB operation of around %94.43 fractional band width. Secondly, the resultant QRHA has another attractive feature of yielding directive pattern of around 30° to 40° for either linear polarizations (H and/or V) and circular polarizations (RHCP and/or LHCP). Furthermore, the gain performance of the final QRHA is around 13 dB that can also be regarded as effective if this antenna is to be used to penetrate through a wall or a ground for a possible TWIR or GPR application. Also, the designed QRHA is directive to be operated effectively in OPIR operation by providing HPBW performances around 30° to 40 ° for LP usages and around 36° for CP usages. These results are in compliance with the results of DRHA design and optimization study that was reported earlier [22].

Conflicts of interest

The authors declare no conflicts of interest.

References

1. Ozdemir, C., & Ling, H. (1997). Joint time-frequency interpretation of scattering phenomenology in dielectric-coated wires. IEEE Transactions on Antennas and Propagation, 45, 1259- 1264.
2. Demirci, S., Ozdemir, C., Akdagli, A., & Yigit, E. (2008). Clutter reduction in synthetic aperture radar images with statistical modelling: An application to MSTAR data. Microwave and Optical Technology Letters, 50, 1514-1520.
3. Ahmed, S. S., Schiessl, A., Gumbmann, F., Tiebout, M., Methfessel, S. (2012). Advanced microwave imaging. IEEE Microwave Magazine, 13, 26-43.
4. Sheen, D. M., McMakin, D. L., & Hall, T. E. (2010). Near-field threedimensional radar imaging techniques and applications. Applied Optics, 49, E83–E93.
5. Yarovoy, A. G., Savelyev, T. G., Aubry, P. J., Lys, P. E., & Ligthart, L. P. (2007). UWB array-based sensor for near-field imaging. IEEE Trans on Microwave Theory and Techniques, 55, 1288–1295.
6. Baranoski, E. J. (2008). Through-wall imaging: historical perspective and future directions. Journal of the Franklin Institute, 345, 556–569.
7. Wang, G. Y., & Amin, M. G. (2006). Imaging through unknown walls using different standoff distances. IEEE Transactions on Signal Processing, 54, 4015–4025.
8. Zhu, F., Gao, S., Ho, A. T. S., Brown, T. W. C., Li, J. Z., & Xu, J. D. (2011). Low-profile directional ultra-wideband antenna for see-through-wall imaging applications. Progress In Electromagnetics Research, 121, 121-139.
9. Dou, Q., Wei, L., Magee, D. R., & Cohn, A. G. (2017). Real-Time Hyperbola Recognition and Fitting in GPR Data. IEEE Transactions on Geoscience and Remote Sensing, 55, 51-62
10. Gu, K., Wang, G., & Li, J. (2004). Migration based SAR imaging for ground penetrating radar systems. IEE Proceedings - Radar, Sonar and Navigation, 151, 317-325.
11. Soldovieri, F., Lopera, O., & Lambot, S. (2011). Combination of Advanced Inversion Techniques for an Accurate Target Localization via GPR for Demining Applications. IEEE Transactions on Geoscience and Remote Sensing, 49, 451-461.
12. Özdemir, C. (2021). Inverse Synthetic Aperture Radar Imaging with MATLAB Algorithms, Second Edition. Wiley. ISBN: 978-1119521334
13. Ghosh, C., Sarkar, T. K. (2009). Design of a wide-angle biconical antenna for wideband communications. Progress in Electromagnetics Research B, 16, 229-245.
14. Tang, X., Li, R., Pei, J., & Long, Y. (2014). An Ultra Wideband Printed Helical Antenna with Low Profile. Progress in Electromagnetics Research Symposium (PIERS), 2014, 1499–1502.
15. Islam, M. A., Istiak, S. M. S., Rahman, I., Tonmoy, S. A. U., & Ali, S. M. R. (2017). Design and Performance Analysis of a Log Periodic Dipole Antenna with a Frequency Range of 1350 to 2690 MHz. Journal of Microwave Engineering and Technologies, 4, 6–12.
16. Kubacki, R., Czyewski, M., & Laskowski, D. (2020). Enlarged Frequency Bandwidth of Truncated Log-Periodic Dipole Array Antenna. Electronics, 9, 1300.
17. Mehdipour, A., Aghdam, K. M., & Faraji-Dana, R. (2007). Completed dispersion analysis of Vivaldi antenna for ultra-wideband applications. Progress In Electromagnetics Research, 77, 85–96.
18. Bruns, C., Leuchtman, P., & Vahldieck, R. (2003). Analysis and simulation of a 1–18 GHz broadband double-ridged horn antenna. IEEE Transactions on Electromagnetic Compatibility, 45, 55–60.

19. Toktas, A. (2016). Log-periodic dipole array-based MIMO antenna for the mobile handsets. Journal of Electromagnetic Waves and Applications, 30, 351-365.
20. Toktas, A. (2016). Scalable notch antenna system for multiport applications. International Journal of Antennas and Propagation, 2016, 1-8.
21. Toktas, A. (2017). G-shaped band-notched ultra-wideband MIMO antenna system for mobile terminals. IET Microwaves, Antennas & Propagation, 11, 718-725.
22. Yılmaz, B., & Özdemir, C. (2017). Design and Prototype of a Compact, Ultra Wide Band Double Ridged Horn Antenna for Behind Obstacle Radar Applications. Turkish Journal of Engineering, 1, 76-81.
23. Novak, L. M, Owirka, G. J., & Netishen, C. M. (1993). Performance of a high resolution, polarimetric SAR automatic target recognition system. Lincoln Laboratory Journal, 6, 11-24.
24. Van Zyl, J. J. (1989). Unsupervised classification of scattering behavior using radar polarimetry data. IEEE Transactions on Geoscience and Remote Sensing, 27, 36- 45.
25. CST. (2012). CST Microwave Studio Advanced Topics. Technical report, CST-Computer Simulation Technology.